Evaluation of SiPM Arrays and Use for Radioactivity Detection and Monitoring

Andrei Semenov, T.Beattie, G.J.Lolos,
Z.Papandreou, M.La Posta, M.Singh,
J.Sanchez-Fortun Stoker, L.Teigrob

(University of Regina)

CAP Congress, June 15, 2015

Talk Outline

- Characteristics of Silicon Photomultipliers (SiPMs), and “classical” evaluation techniques when photoelectron peaks can be resolved in ADC spectrum.
- New techniques of measurement of the PDE, the cross-talk probability and the breakdown voltage for the SiPM-arrays with summed output (when individual p.e. peaks can not be separated).
- SiPM-based compact detectors for monitoring of gammas and thermal neutrons.

Silicon Photomultiplier (SiPM)

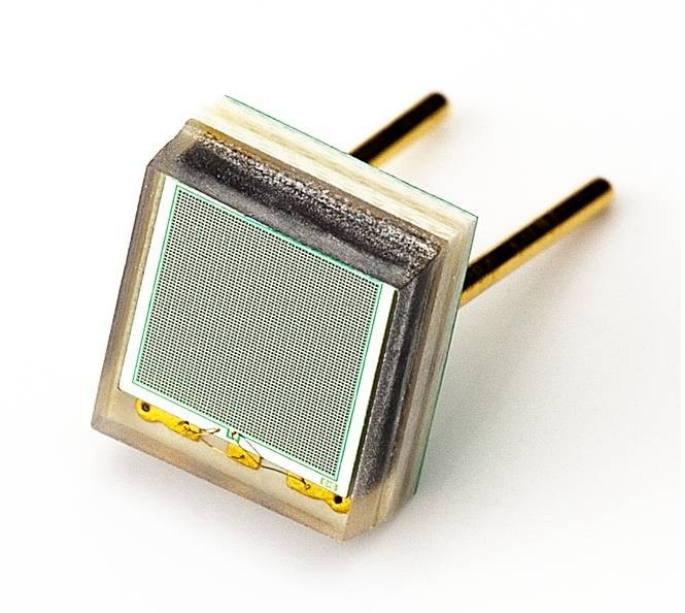

Matrix of avalanche photodiodes (APDs) built on the same Si substrate

Reverse bias

Avalanche (Geiger) operation mode: bias above breakdown voltage

SiPM is few mm in size

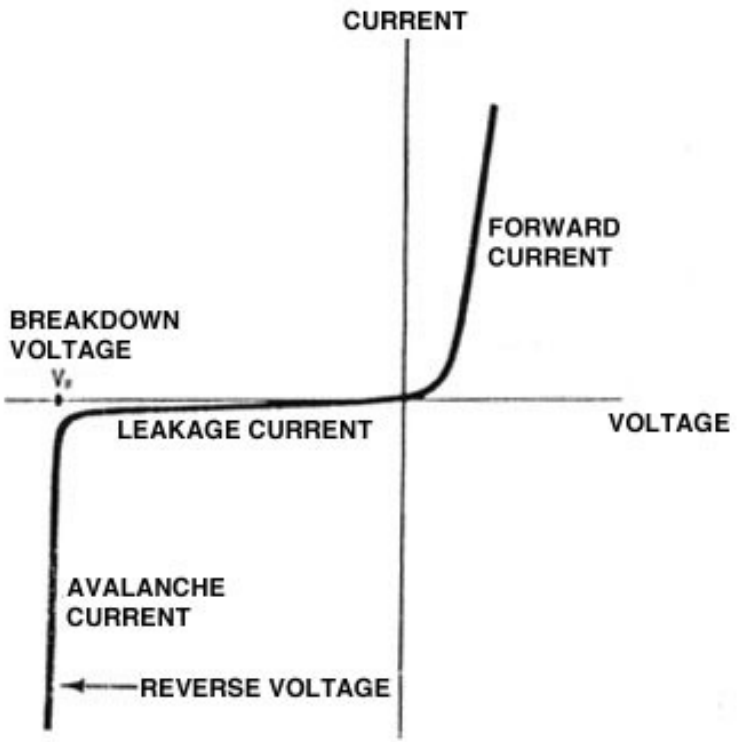

SiPM Properties

- Single photon sensitive device (PDE~20-30%)
- Although each APD is a “digital” device, photon flux fires many APDs

  ⇒ “analog” SiPM signal
- Low bias voltage (20-70 V to be compared with 1.5-2 kV for PMTs: safety, bulk and cost of HV cables compared to low voltage operating requirements of the SiPM’s)
- A few μm-thick depletion layer ⇒ High electric field ($\sim 3\times10^5$ V/cm)
- High gain (of $\approx 10^6$). Stable & fast signal
- No sensitivity for magnetic field. (A few Tesla field is no problem.)

Gain Calibration with Photoelectron Peaks

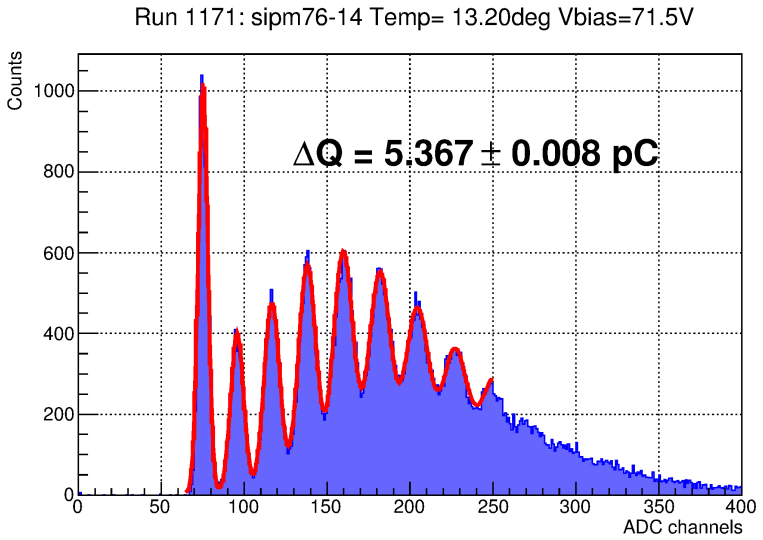

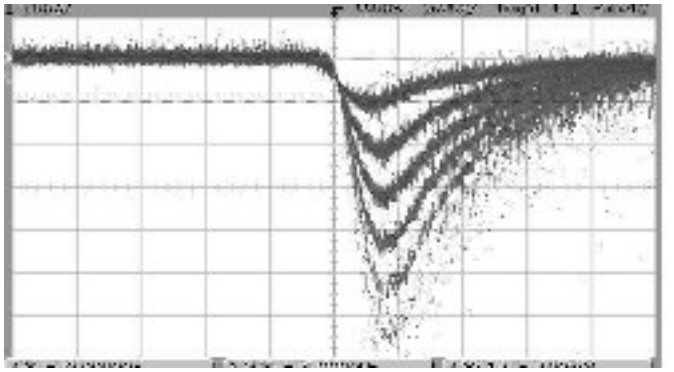

Energy resolution is good enough to resolve individual p.e. peaks

$$\Delta Q = C_p \bullet (V_{bias} - V_{break})$$

$$Gain = \Delta Q / e$$

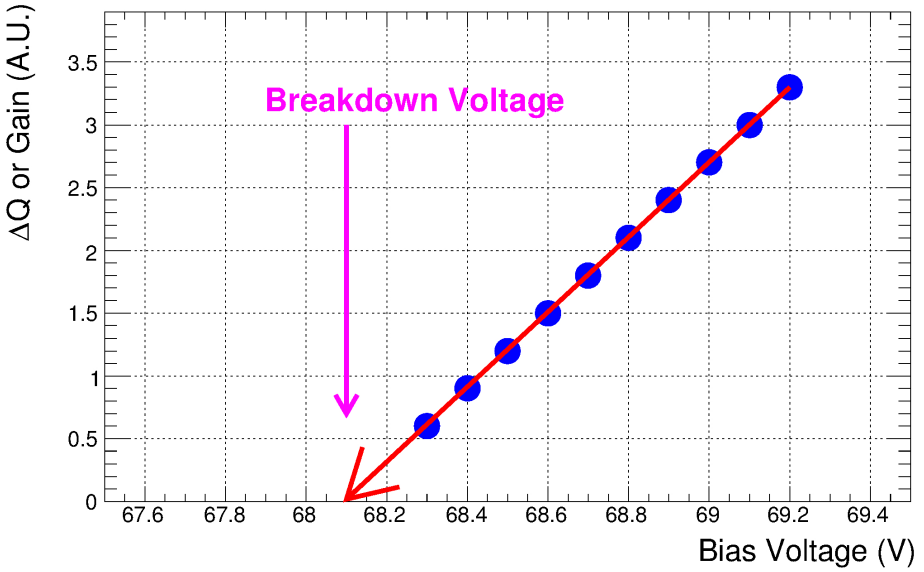

Gain Drift with Temperature

The gain is quite sensitive to the temperature at a given bias voltage.

The primary reason is that the breakdown voltage varies with temperature; a linear increase in breakdown voltage of 20-60 mV/°C is generally observed (with significant sensor-to-sensor variation).

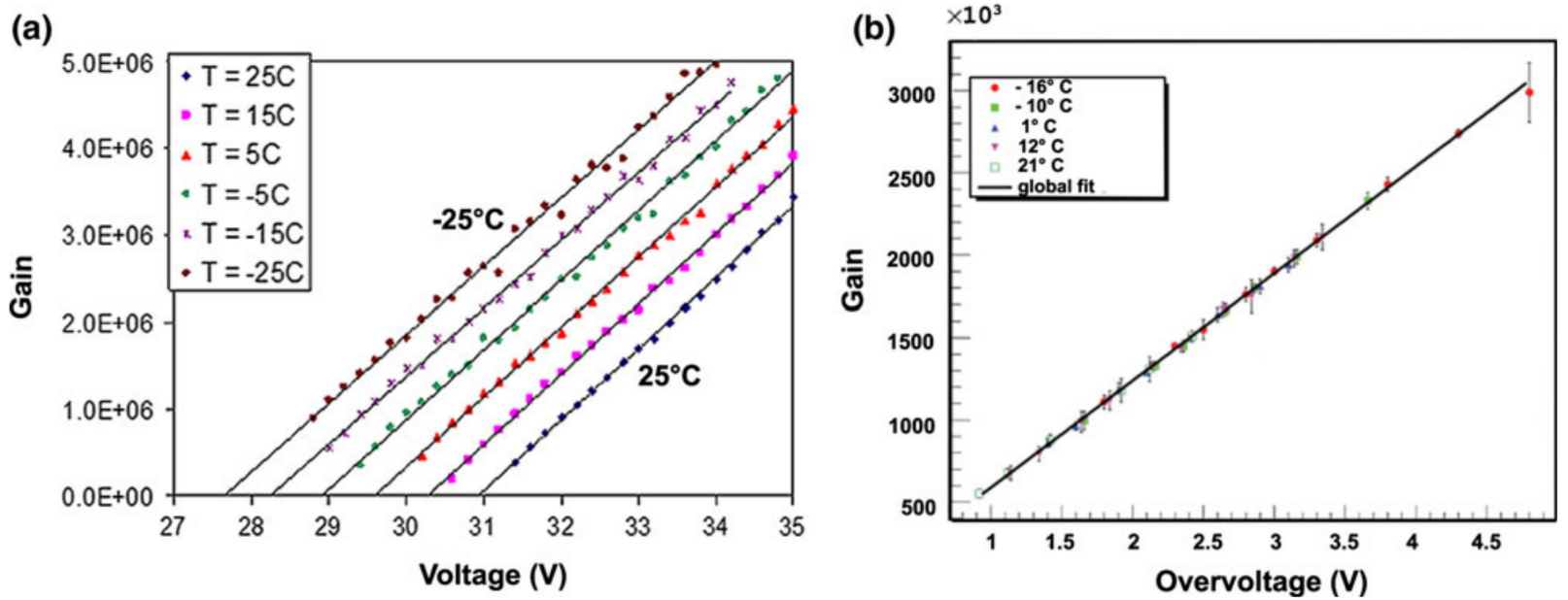

(a) Variation of gain as a function of bias voltage for a 1 × 1 mm^2 SiPM with 400 cells, at different temperatures (from left to right: −25, −15, −5, 5, 15, and 25 °C) Piemonte *et al.*[71] © 2008 IEEE. (b) Gain as a function of overvoltage for different temperatures for a 1 × 1 mm^2 SensL SPM. Ramilli[72] © 2008 IEEE.

Photodetection Efficiency (PDE)

A probability to detect a single photon:

$$PDE = FF \cdot P_g \cdot QE$$

Quantum efficiency (>80% for silicon): strongly wavelength dependent and temperature dependent.

Probability of Geiger discharge (0.5-1.): depends on the location of the primary electron-hole pair and electrical field shape, and increases with overvoltage. Competing processes are recombination etc.

Fill factor (20-80%): a constant parameter inherent to the geometry of the device (the microcells are surrounded by a dead area).

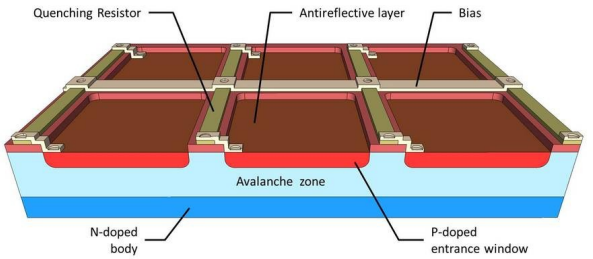

Measurements of PDE

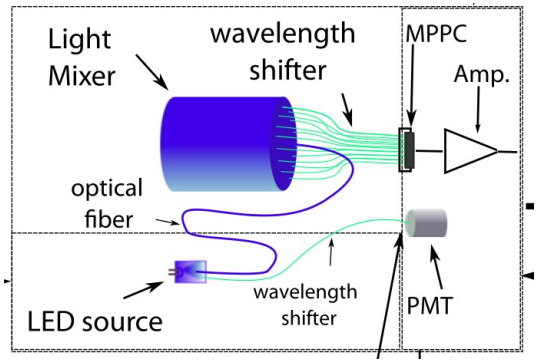

$$PDE \approx - ln(Prob(0)) / N_\gamma$$

Mean number of incident photons (from calibrated PMT or photodiode monitors)

Mean number of avalanches
(from Poisson-distributed spectrum)

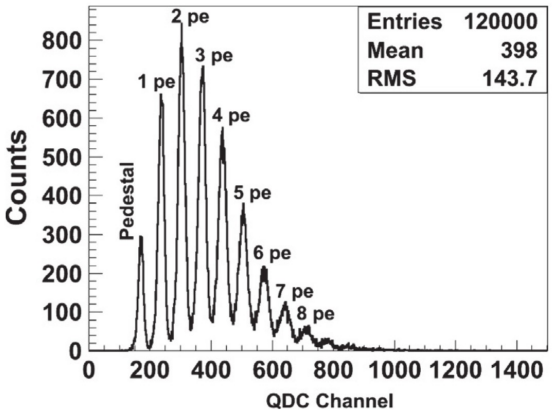

O.Soto et al., NIM A739, 89

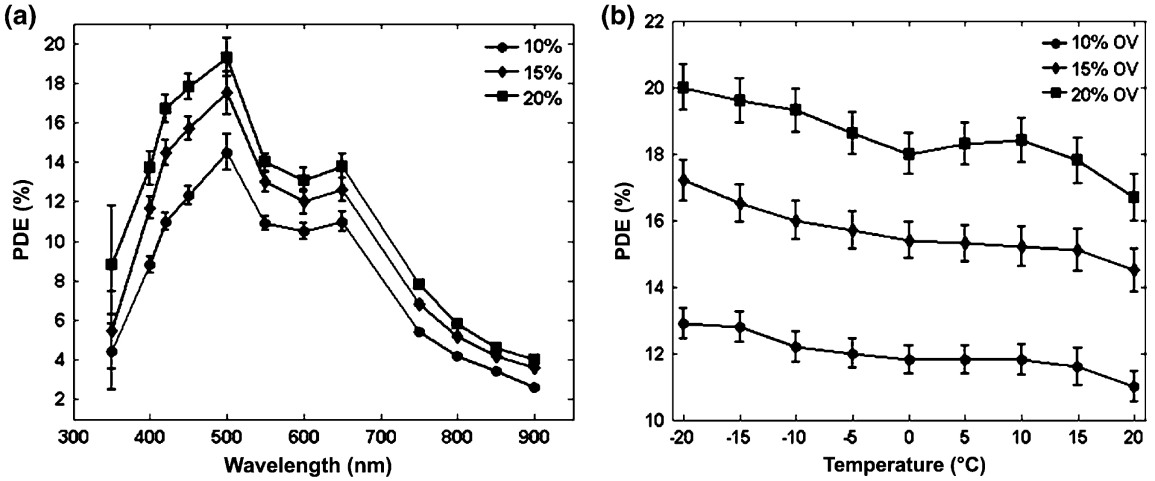

(a) PDE spectra for different overvoltages (10, 15, and 20%) acquired with a 1 × 1 mm^2 SiPM (STMicroelectronics) with 289 cells and a fill factor of 48%. Mazillo *et al.*[49] © 2009 IEEE. (b) PDE as a function of temperature for different overvoltages (10, 15, and 20%) for the same device as (a). Mazillo *et al.*[49] © 2009 IEEE.

Noise

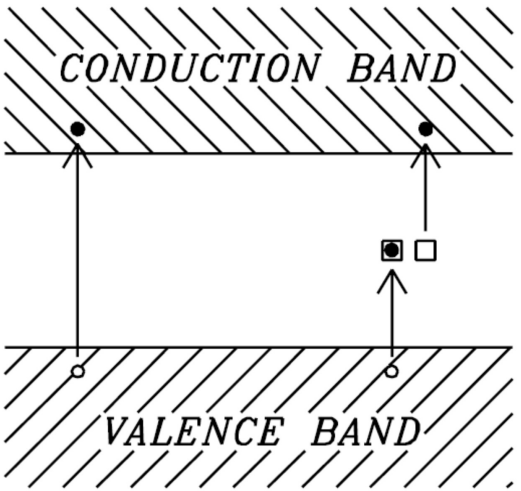

O.Soto et al., NIM A739, 89

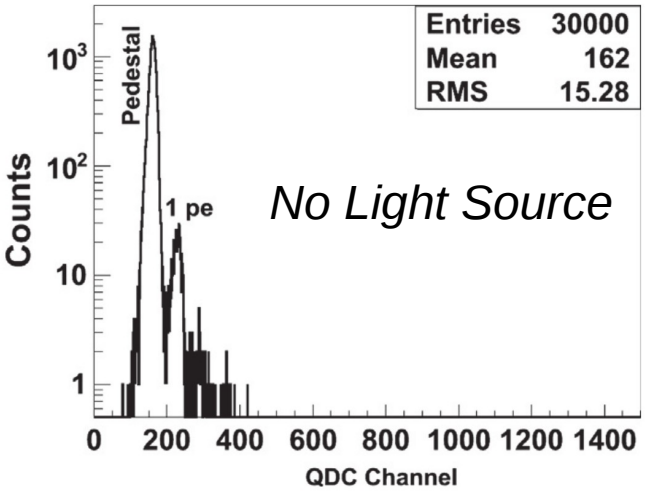

Main source of noise is thermally generated (viz., electron-hole pair is created by thermal exitation). Electronic noise is negligible because of the high gain of SiPM (very different situation compared to APD).

Dark count rate ranges from around 1 Mhz/mm^2 at room temperature to a few kHz/mm^2 at -20C; most dark pulses have an amplitude of 1 p.e.

In medical imaging, the photon fluence from the scintillator is usually high and short integration times are used, so generally thermal noise is not a major limiting factor. **However, it may degrade performance of the systems that determine position measuring light-spread function.**

Optical Cross-Talk

Optical photons can be produced within a G-APD cell (≈ 3×10^{-5} photons per electron crossing the junction) and can potentially move to a neighboring cell and trigger avalanche that will be indistinguishable from the true signal.

Optical cross-talk probability (CTP) varies between 1 and 50% for different structures and different overvoltages. If not corrected for, optical cross-talk can result in overestimation of the PDE.

To reduce cross-talk, cells need to be optically isolated (larger pitch between cells or trenches filled with an opaque material between the cells).

Extraction of CTP is based on a statistical model that predicts deviation of the relation between the mean and variance of measured spectra:

$$Mean = \langle N \rangle (1 + CTP) ; \qquad Var = \langle N \rangle (1 + 3\times CTP + CTP^2)$$

from that is expected from Poisson distribution.

Afterpulsing

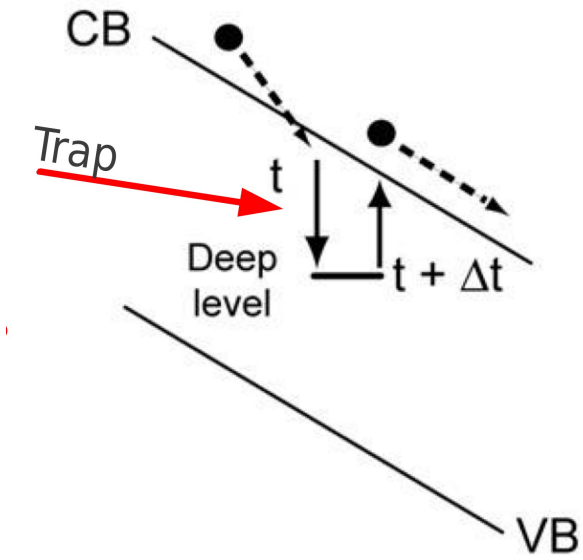

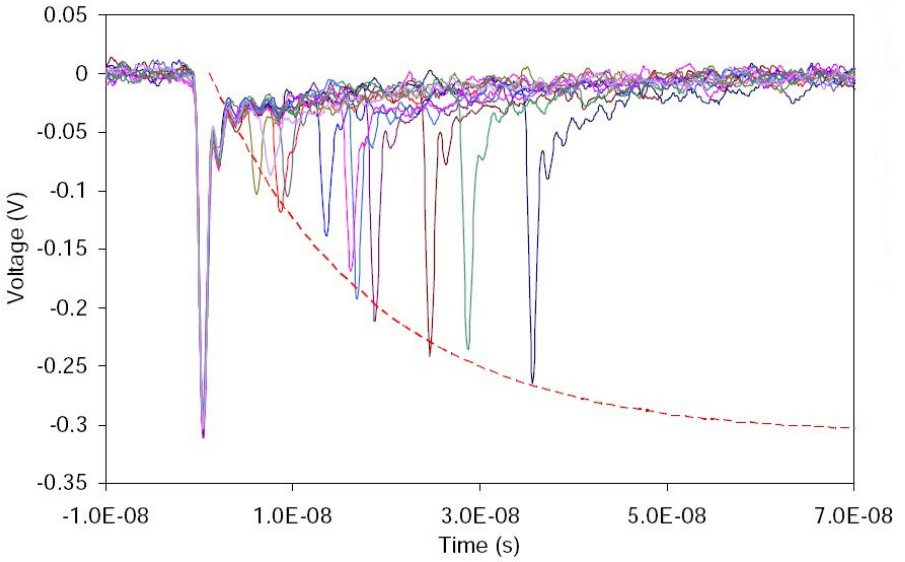

Charge carrier can be trapped at impurities during the Geiger discharge and released after a certain delay. The incidence varies with overvoltage between 0.3 and 10%, and depends on the cell recovery time and temperature (sharp increase below 120K).

Afterpulsing can lead to a single scintillation event producing 2 pulses that are separated in time from a few tens of ns to a few µs.

If ADC gate is comparable with SiPM pulse duration, afterpulse contribution in ADC spectrum is small.

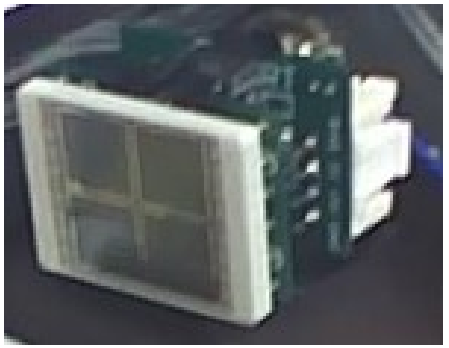

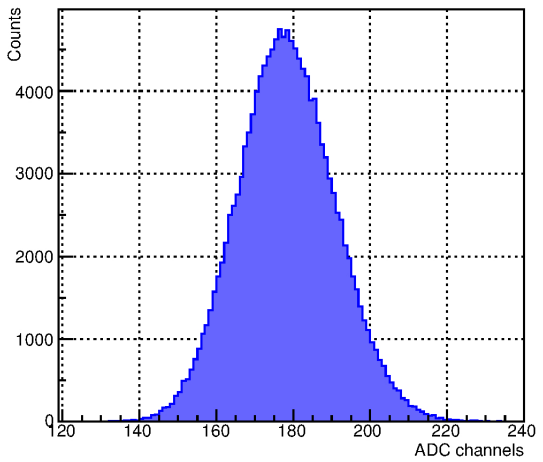

SiPM Array

a.k.a. Multi-Pixel Photon Counter (MPPC)

To provide a bigger-area photodetector, a few SiPMs (typically, 9-16) might be combined in the SiPM array.

Although each SiPM in the array may have an individual output pin, producers often sell the detector with attached small-in-size pre-amplifier with one “summed” output.

Higher dark current (noise) from the summed SiPMs as well as some variations in the gain make the photopeaks wider and indistinguishable in the shape of ADC spectrum.

New evaluation techniques are needed!

Breakdown Voltage from IV Curves

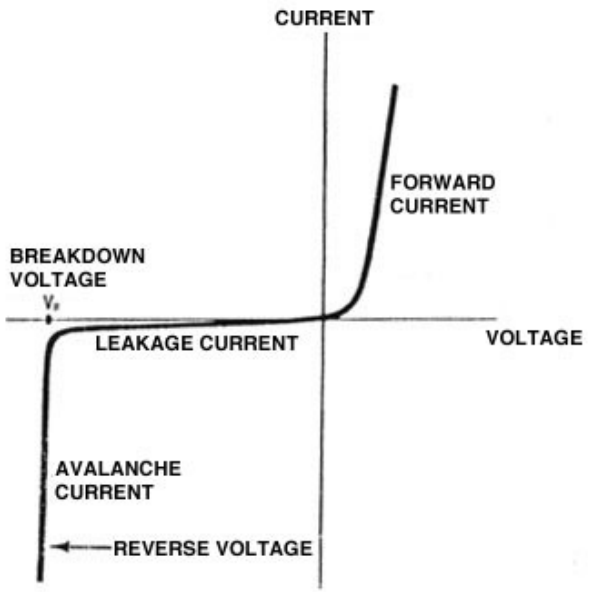

- **Measure the dark current as a function of bias voltage**
- **Fit the "Leakage Current" region with a linear function (Ohm's Law), and find the voltage where the deviation in avalanche region starts**

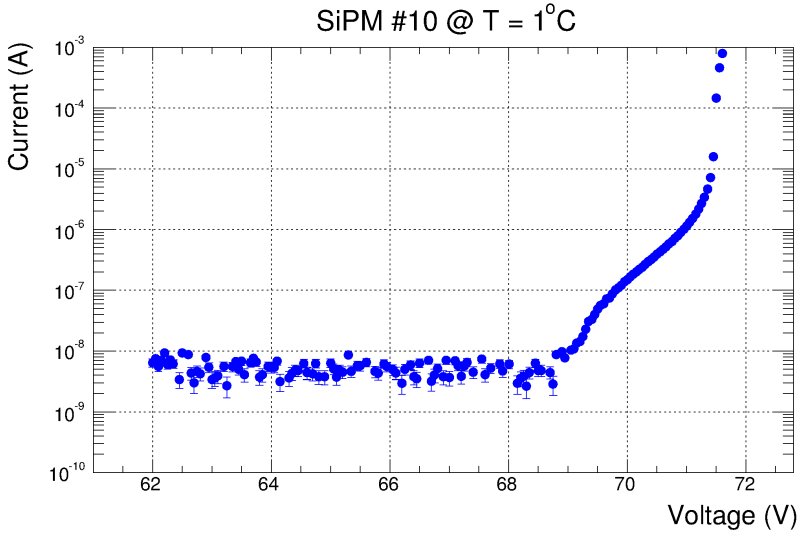

Problems: Big fluctuations and (sometimes) no-Ohm's-law behaviour

Solution: 30-45 min. of SiPM "warming"

Hamamatsu S12045(X) MPPC
(Multi Pixel Photon Counter)

Array of 16 3×3 mm² SiPMs

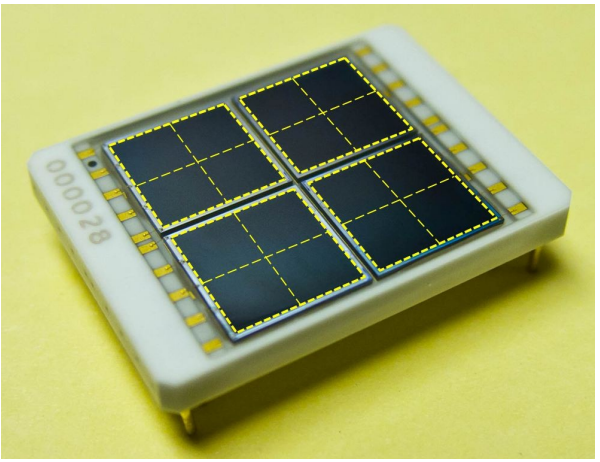

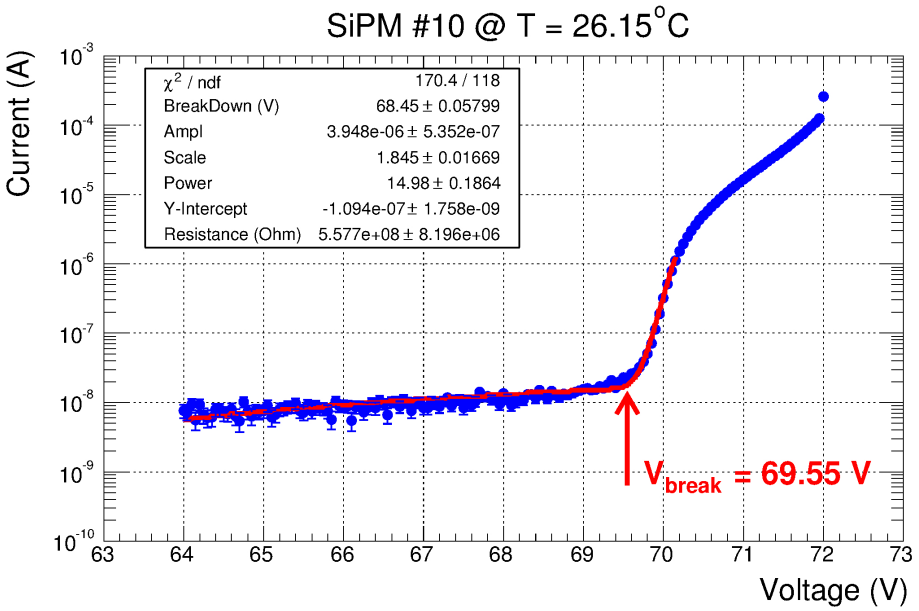

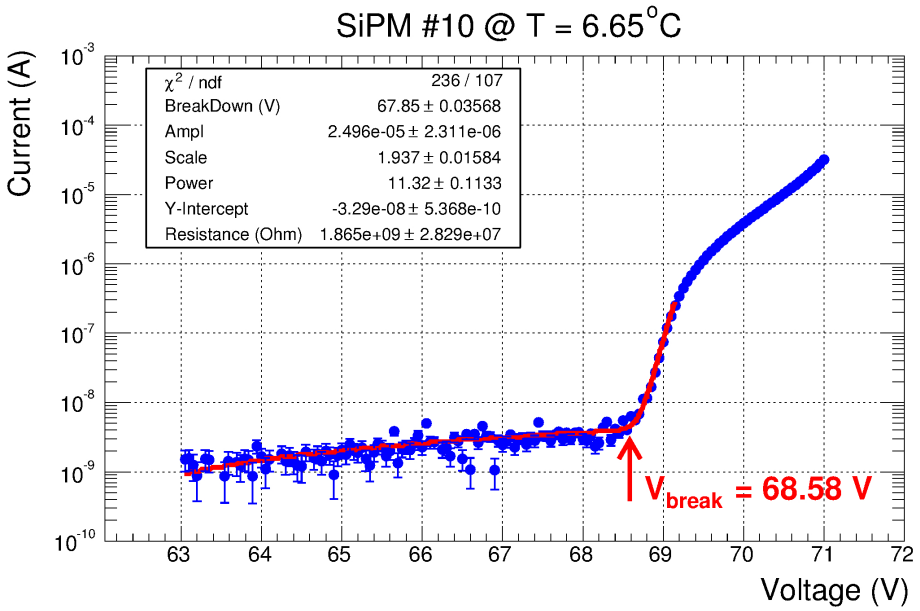

Measurements were done at different temperatures with Keithley 6471 picoammeter/voltage source

“IV-Curves” and “Photoelectron-Peaks” Results Comparison

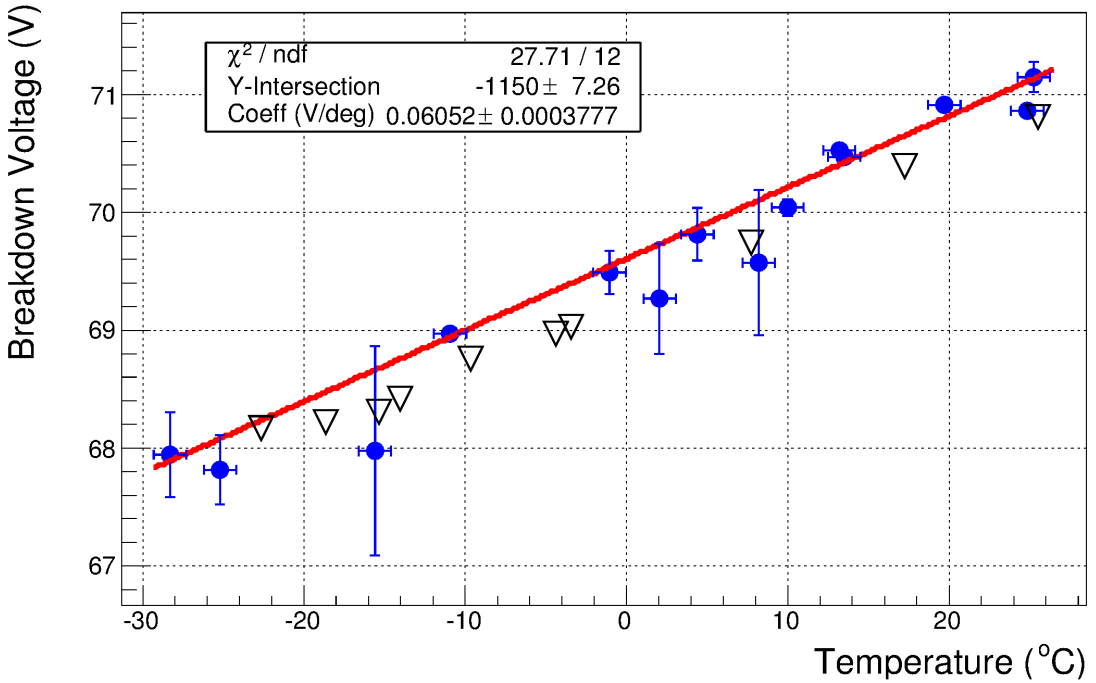

Blue circles for IV-Curve method

Empty triangles for p.e.-peak method (cross-check on one cell using 16-output testing board from Jefferson Lab)

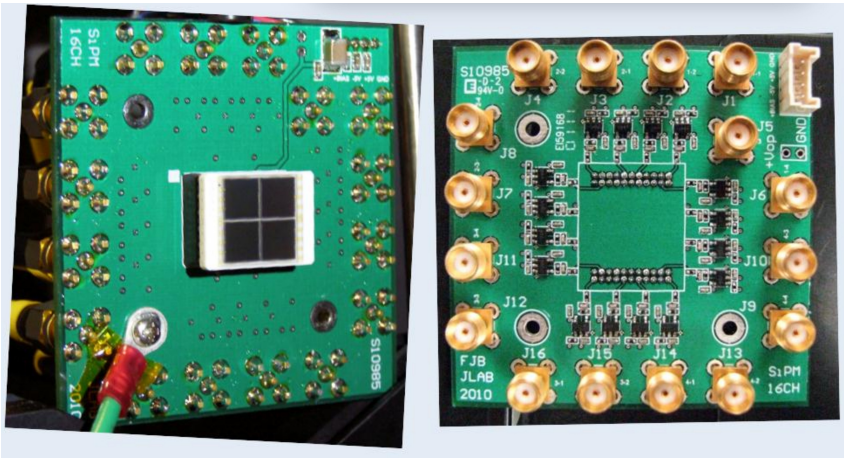

Slope of about 60 mV/deg

(good agreement for both methods)

Measurement of PDE (Setup)

Hamamatsu S12045(X) MPPC

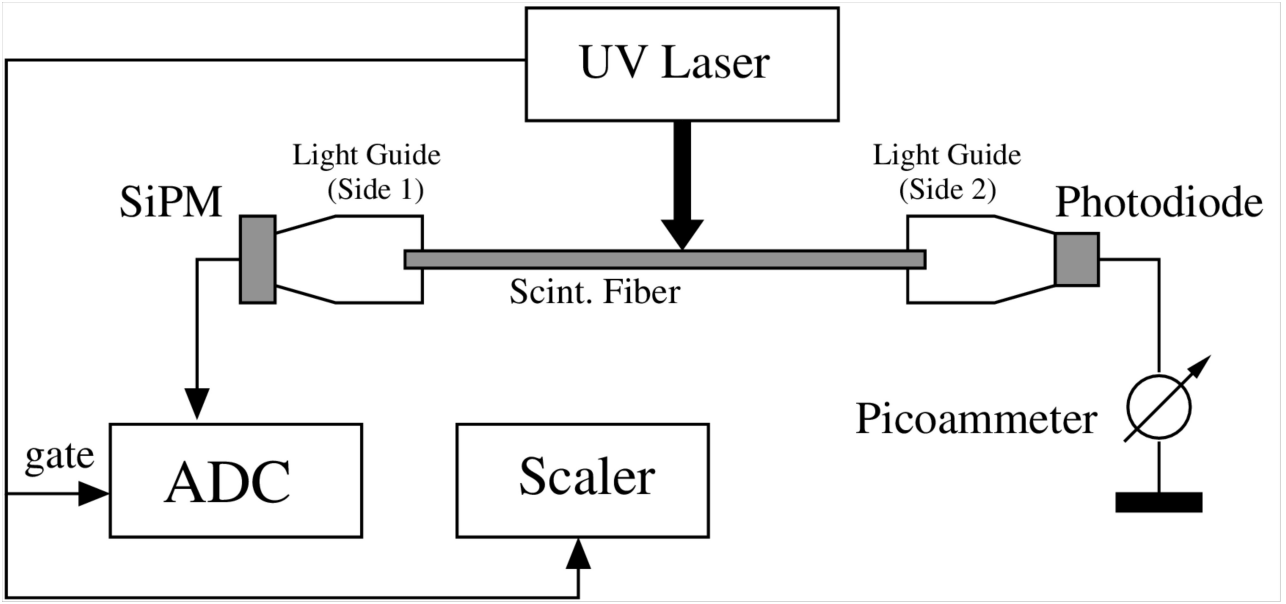

- *Fast UV laser (PicoQuant PDL 800-B pulsed diode laser) stimulates scintillation fiber at its center; (statistically) equal amount of light propagates through light guides to both sides of symmetric setup;*
- *Frequency of the laser is controlled by scaler*
- *Output signals from the SiPM array at one side are sent to ADC*
- *Keithley 6487 picoammeter measures the current from the calibrated Hamamatsu S2281 photodiode on another side to estimate an average number of photons arrived at each side*

Measurement of PDE (Number of Photons)

Scintillation fiber wavelength spectrum *g(λ)* was measured with USB4000 spectrophotometer and convoluted with photodiode spectral sensitivity *S(λ)* and the photon energy *E(λ)=hc/λ* as follows:

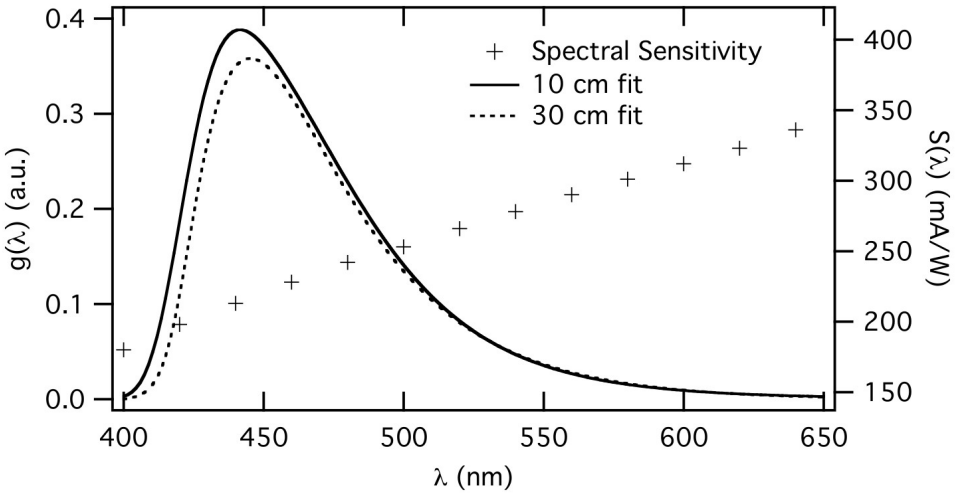

$$\overline{Q} = \frac{\int_0^\infty [E(\lambda) \cdot g(\lambda) \cdot S(\lambda)]\, d\lambda}{\int_0^\infty g(\lambda) d\lambda}$$

to yield the average charge per photon, *Q*. The average number of photons was then determined as follows:

$$\overline{N_\gamma} = \frac{I - I_{dark}}{\overline{Q} \cdot f_{laser}}$$

Measurement of PDE (Statistical Model)

$$f(x-m_n) = k_0 \sum_{N_\gamma=0}^{N_\gamma^{max}} \mathcal{P}(N_\gamma, \overline{N}_\gamma) \left[\sum_{N_a=0}^{N_\gamma} \mathcal{B}(N_a, N_\gamma, k_1) \left(\sum_{N_{ct}=0}^{N_a} \mathcal{P}(N_{ct}, \epsilon_{ct} N_a)\, \mathcal{G}(x-m, k_2(N_a+N_{ct}), \sigma_p) \right) \right]$$

Distribution of photons from the fiber

Photons-to-avalanches conversion with ***PDE=k_1***

Acconting for optical cross-talk with CTP=ε_{ct}

"Smearing" of p.e. peaks with the width of noise dist σ_p

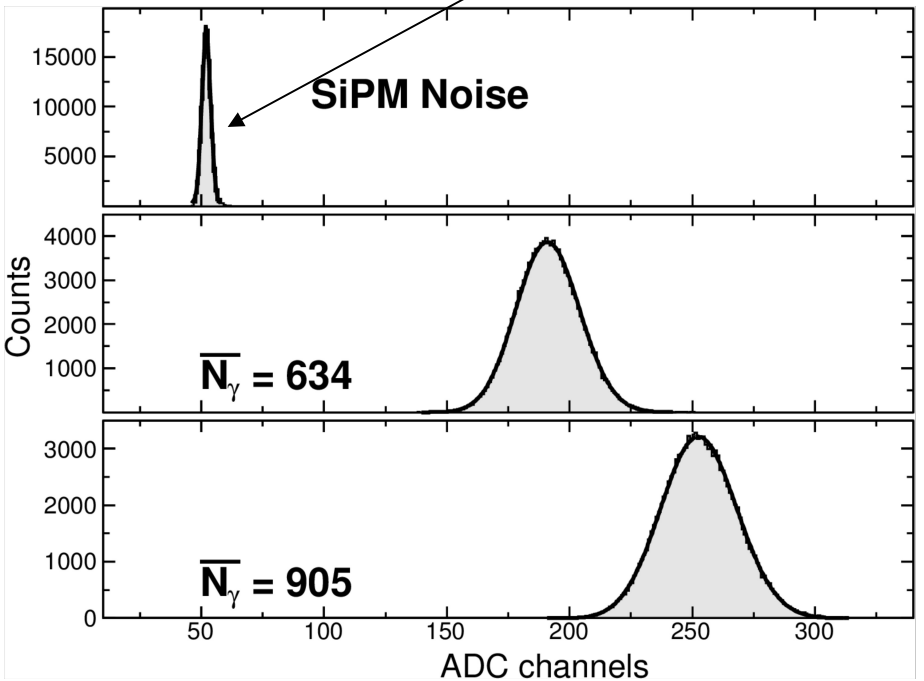

Cross-talk probability ε_{ct} was measured for this SiPM model in the Universidad Tecnica Federico Santa Maria (Chile).

Measurement of PDE (Results)

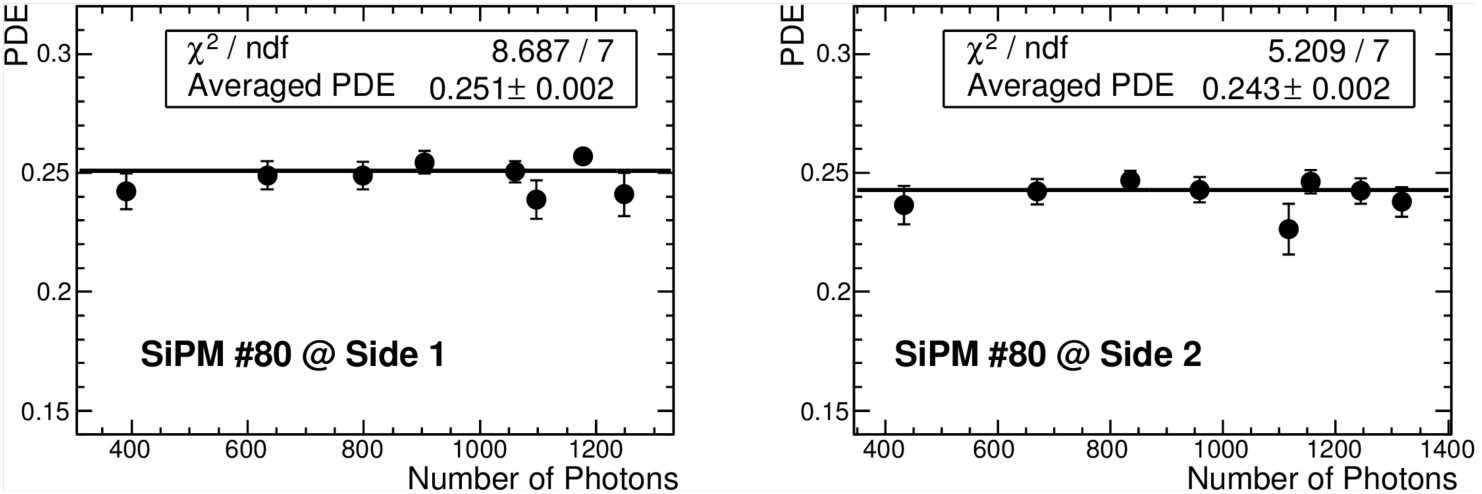

Results demonstrate stability over a wide range of illumination (viz., no non-linearity effects).

Measurements were repeated after swapping the photosensors from one side to the other.

Ratio of PDE results before and after swapping indicates that the apparatus is symmetric in average, but in a single measurement, asymmetries in the light on side 1 and side 2 up to 10% are possible that contributes as 5% systematic error in to the final result.

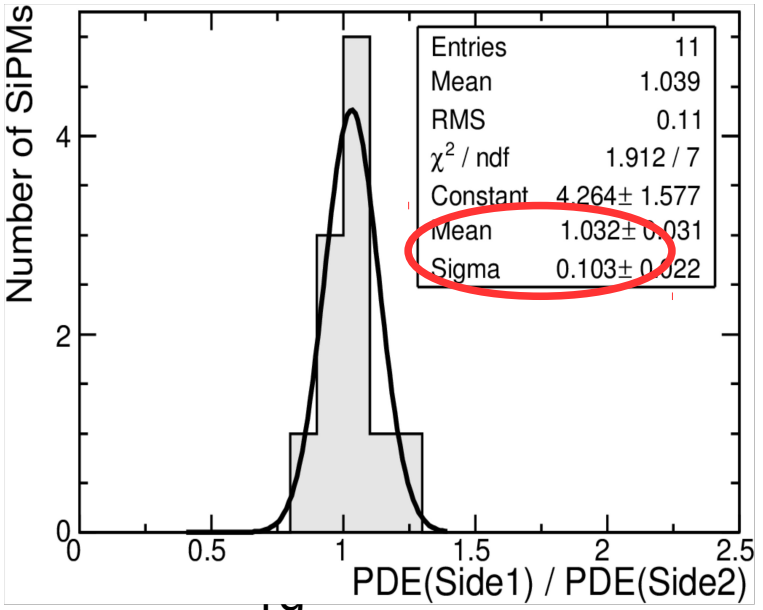

Measurement of PDE (Results)

Geometrical mean of the results from both sides is histogrammed for 11 SiPM arrays that were tested.

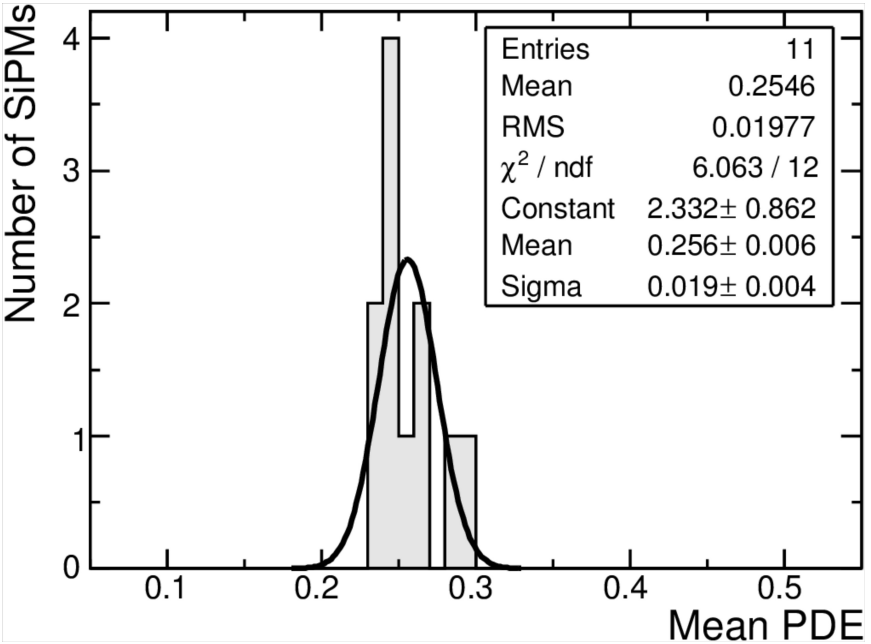

Results are in a very good agreement with PDE measured for this type SiPMs with traditional "photoelectron-peak" technique by our Chilean colleagues.

Uncertainty from CTP

The value of cross-talk of (*0.133±0.015*) was obtained from the work of our Chilean colleagues (*O.Soto, NIM A739, 89*) for the conditions of our measurements

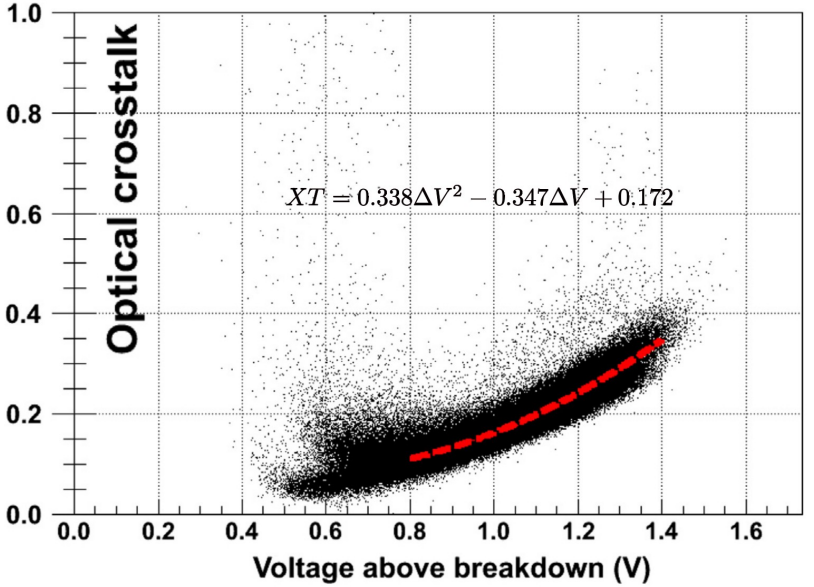

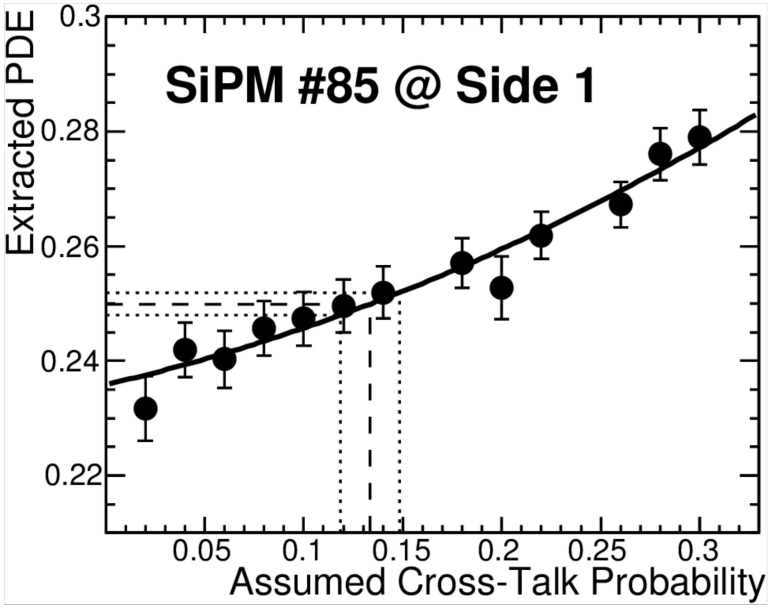

We examined our sensitivity to this parameter by varying the CTP value in our fits (note rising PDE-vs-CTP dependence).

Uncertainty in used CTP results in less than 1% systematic uncertainty in the absolute value of PDE.

Independent Measurement of CTP

Alternatively, we can estimate PDE from the charge of output pulses from SiPM array:

$$PDE = \frac{1}{\bar{N}_\gamma} \times \frac{(ADC - ADC_p) \times q_{ch}}{(1 + CTP) \times e \times Gain}$$

This falling *PDE-vs-CTP* dependence is shown in the solid red line;
the crossing with the (black) line from "statistical" method provides absolute independent values of PDE and CTP.

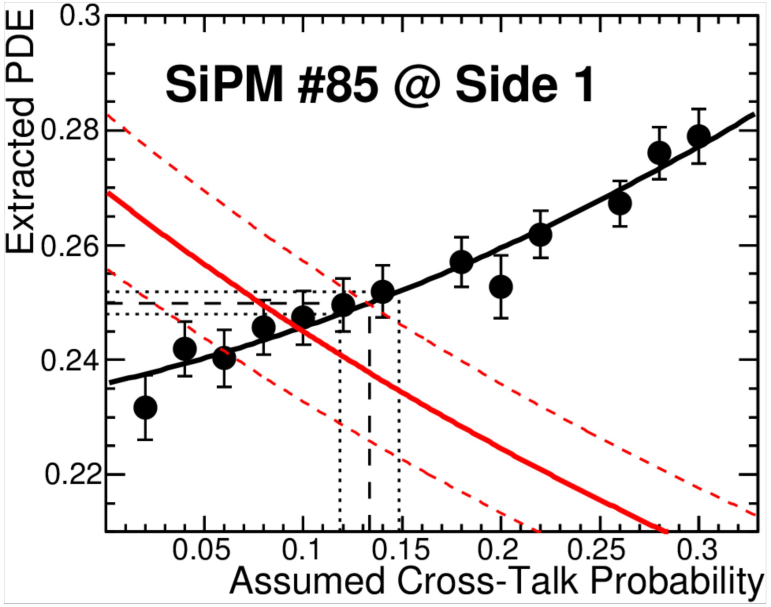

Extracted CTP is in a decent agreement with the value from Chile measurements.

The red dashed lines correspond to ±5% uncertainty on ADC calibration q_{ch}=*0.25 pC/ch* provided by vendor for this ADC model.

Accurate calibration of our ADC module can improve accuracy of CTP extraction.

Summary on Evaluation Techniques:

- *Operation of SiPM-based detectors for imaging (viz., detector response stability and uniformity as well as a possible desire to decrease the noise via cooling) and personal radiation safety (viz., outdoor use and sometimes low signal) requires temperature control and bias/voltage correction.*

- *Sensor-to-sensor variation of the dependence on temperature suggests evaluation of each SiPM array.*

- *We have developed novel techniques for independent measurement of the breakdown voltage, PDE and CTP without using ADC photoelectron peaks that are unavailable for SiPM arrays with output summed over all cells. Cross-check of these techniques against traditional photoelectron-peak methods demonstrates a good agreement.*

Compact Gamma Detector

Objective: Create a prototype of compact and inexpensive gross counting gamma counter for the first responders that can reliably detect a gamma-source flux above the noise and natural background rates.

Realization: Small 10×10×50 mm^3 plastic scintillator viewed by 3×3 mm^2 SiPM (the choice is driven by the cost and required portability).

Challenges: Low efficiency to the gammas of the plastic scintillator and a need to transport the light from 10×10 mm^2 scintillator cross-section to the 3×3 mm^2 SiPM window (potential loss factor of 11).

Solution: Optimization of the reflector around the scintillator.

Result: The best found reflector is a teflon tape.

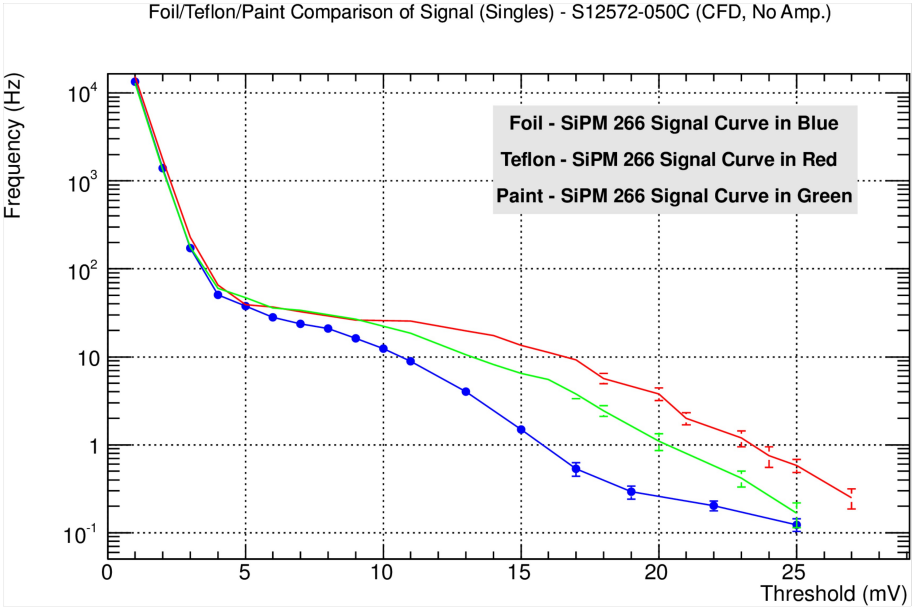

Compact Gamma Detector

Blue: ^{60}Co (E_γ=1.17 MeV, 1.5×10^3 Bq)

Red: ^{133}Ba (E_γ=356 keV, 7.6×10^3 Bq)

Green: ^{241}Am (E_γ=60 keV, 3.6×10^5 Bq)

Black: Natural background and cosmics

Magenta: SiPM noise

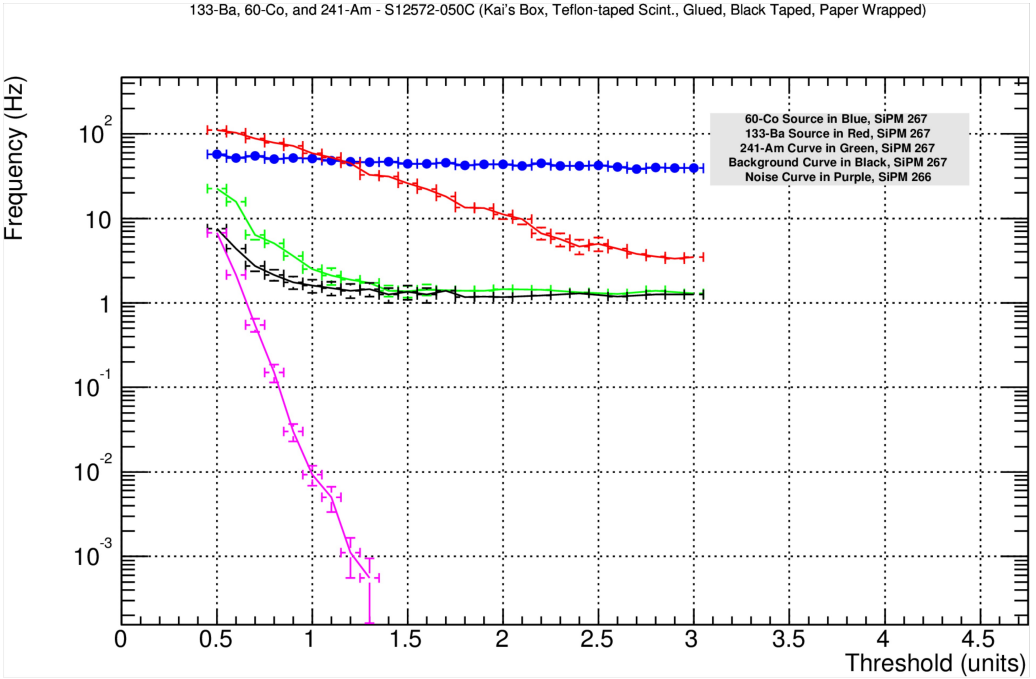

Reliable (well above the natural background) and inexpensive detection of gammas with energy > 300-400 keV

No efficiency loss because of the light collection for the gammas with energy > 1 MeV that converted in the scintillator

Compact Detector of Thermal Neutrons

- ^{3}He is a standard for neutron detection: large cross-section to capture thermal neutrons (0.025 eV):

$$n + {}^{3}He \rightarrow {}^{3}H + p + 0.765\ MeV\ (5400\ barn)$$

- Problem: Shortage of world supply of ^{3}He (by-product from beta-decay of tritium from nuclear weapon stockpiles)
- Compact detector based on thermal neutron capture by ^{10}B (3840 barn):

$$n + {}^{10}B \rightarrow {}^{7}Li^{*} + \alpha + 2.3\ MeV\ (94\%)$$
$$\rightarrow {}^{7}Li + \alpha + 2.8\ MeV\ (6\%)$$

- WLS fiber is covered with ZnS and ^{10}B-enriched B_4C
- Readout with 1×1 mm^2 SiPM
- Control measurement with the fiber covered with ZnS only

Compact Detector of Thermal Neutrons

- ➔ Am-Be generator (thermal neutrons + 2-MeV gammas)
- ➔ Blue spectrum: WLS fiber covered with ZnS+B4C (neutron sensitive)
- ➔ Red spectrum: WLS fiber covered with ZnS only (neutron insensitive)

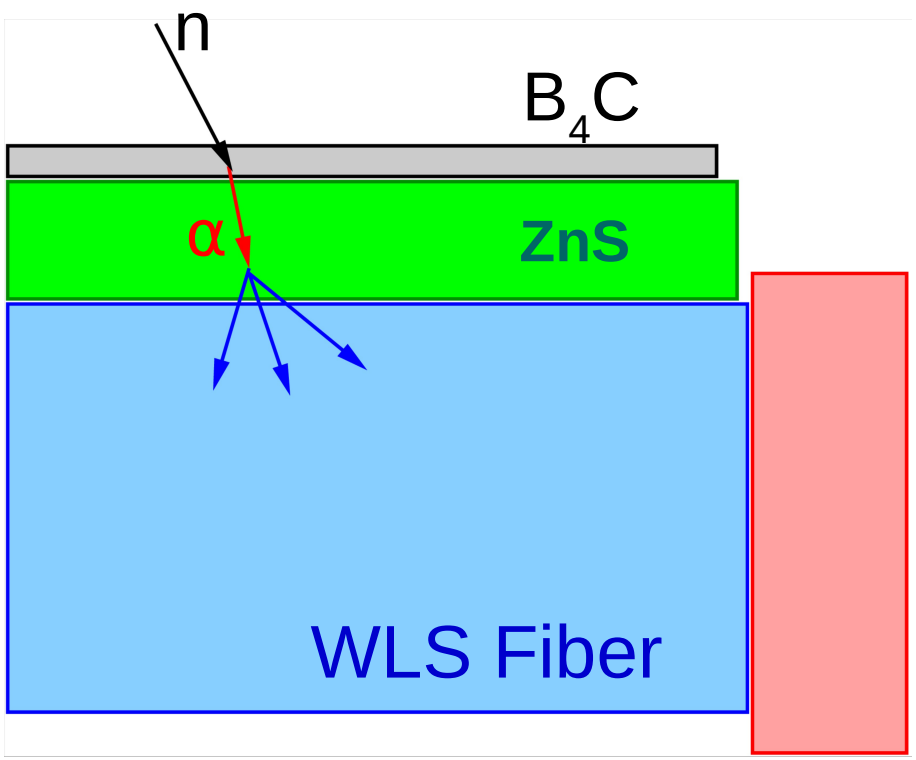

1×1 mm² SiPM

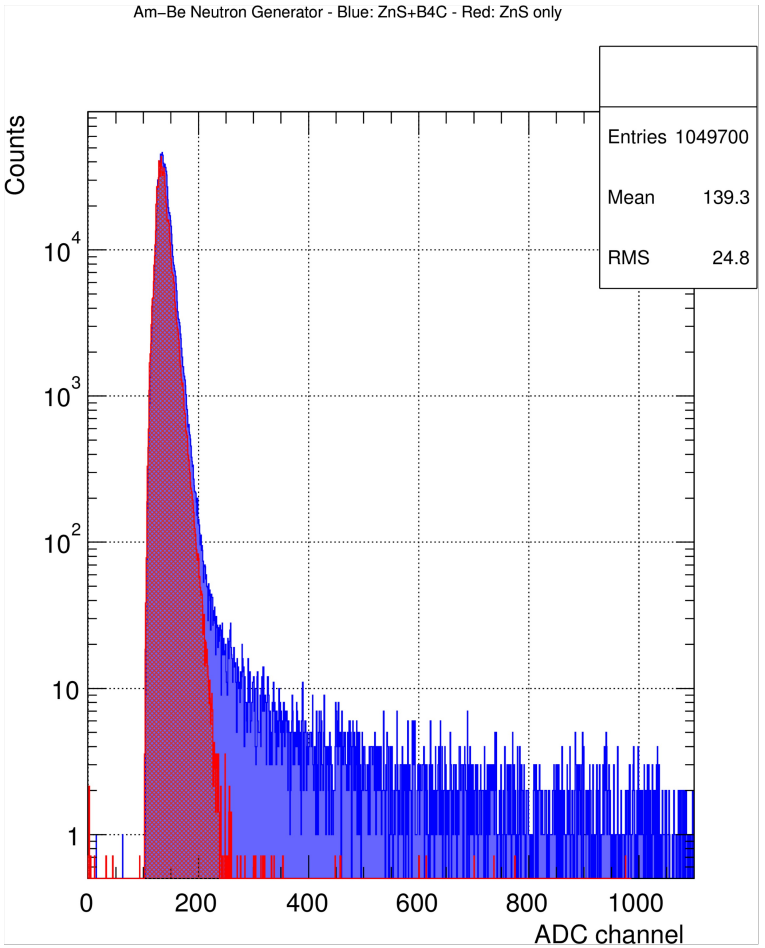

Acknowledgements

- Fedoruk Centre
- NSERC
- Partners from Jefferson Lab and Chile
- Kai Kaletsch
- SPARRO group team
- UofR Summer students